Published in final edited form as:
J Microsc. 2012 July ; 247(1): 10–22. doi:10.1111/j.1365-2818.2011.03572.x.

The characean internodal cell as a model system for studying wound healing

I. Foissner and **G.O. Wasteneys**
Cell Biology/Plant Physiology, University of Salzburg, Austria and Department of Botany, University of British Columbia, Vancouver, BC, Canada

Summary

This work describes the characean internodal cell as a model system for the study of wound healing and compares wounds induced by certain chemicals and UV irradiation with wounds occurring in the natural environment. We review the existing literature and define three types of wound response: 1) cortical window formation characterized by disassembly of microtubules, transient inhibition of actin-dependent cytoplasmic streaming and chloroplast detachment, 2) fibrillar wound walls characterized by exocytosis of vesicles carrying wall polysaccharides and membrane-bound cellulose synthase complexes coupled with endocytosis of surplus membrane and 3) amorphous, callose- and membrane-containing wound walls characterized by exocytosis of vesicles and endoplasmic reticulum (ER) cisternae in the absence of membrane recycling. We hypothesize that these three wound responses reflect the extent of damage, probably Ca^{2+} influx, and that the secretion of Ca^{2+} - loaded ER cisternae is an emergency reaction in case of severe Ca^{2+} load. Microtubules are not required for wound healing but their disassembly could have a signalling function. Transient reorganization of the actin cytoskeleton into a meshwork of randomly oriented filaments is required for the migration of wound wall forming organelles, just as occurs in tip-growing plant cells. New data presented in this study show that during the deposition of an amorphous wound wall numerous actin rings are present, which may indicate specific ion fluxes and/or a storage form for actin. In addition, we present new evidence for the exocytosis of FM1-43-stained organelles, putative endosomes, required for plasma membrane repair during wound healing. Finally we show that quickly growing fibrillar wound walls, even when deposited in the absence of microtubules, have a highly ordered helical structure of consistent handedness comprised of cellulose microfibrils.

Keywords

Actin cytoskeleton; Ca^{2+}; callose; cellulose; cell wall; *Chara*; exocytosis; endocytosis; endoplasmic reticulum; *Nitella*; plant; stress

Introduction

The ability to heal wounds is essential for the survival of organisms, and is especially well developed in sessile plants, which are unable to escape biotic or abiotic stress. In plant cells, rapid deposition of a wound wall is required to repair mechanical damage and plays an important role in the defense against pathogens (e. g. Hardham *et al.*, 2007). Apart from the obvious economic importance of plant defense systems, the study of wound healing has

Correspondence to: Ilse Foissner, Dept. Cell Biology, Div. Plant Physiology, University of Salzburg, Hellbrunnerstrasse 34, A-5020 Salzburg, Austria. Tel. 0043 662 8044 5553; fax 0043 662 8044 619; ilse.foissner@sbg.ac.at.

Europe PMC Funders Author Manuscripts

greatly improved our understanding of biological principles (Nagai, 1993) and serves as a model for the investigation of various cellular processes (Menzel, 1988).

The Characeae are multicellular green algae (Fig. 1A) that are considered to be closely related to the lineage that gave rise to land plants (Qiu *et al.*, 2008). Their multinucleate internodal cells can attain a length of up to 20 cm. Their simple cylindrical shape and large size, as well as the excellent imaging conditions made them a useful model system for various research fields (Braun *et al.*, 2007). They are famous for their rapid cytoplasmic streaming and therefore attractive for studying the actin cytoskeleton (Williamson *et al.*, 1989; Foissner & Wasteneys, 2000a; Braun *et al.*, 2007). They have also been important for the elucidation of microtubule properties (Wasteneys & Williamson, 1989 and references therein). In addition, internodal cells are convenient for studying various aspects of membrane properties (Tazawa & Shimmen, 2001) as well as those of the cell wall (Proseus & Boyer, 2006; Wei & Lintilhac, 2007).

Death of the giant internodes causes considerable loss of cytoplasmic biomass and severe damage to the thallus (Menzel, 1988). Probably for that reason, characean internodes, like other coenocytic algae, have developed an effective wound healing mechanism that makes them an excellent system for studying various aspects of wound repair (Menzel, 1988). In this article we review the existing literature about structural and dynamic aspects of wound healing in characean internodal cells and present so far unpublished data which shed new light on the formation and function of different wound walls. Details about wounding-induced electrophysiological responses are found elsewhere (e.g. Shimmen, 2008).

Materials and methods

Plant material, culture conditions and wounding

Shoots of *Nitella flexilis* L. (Ag.), *Nitella pseudoflabellata* A.Br., em. R.D.W., *Nitella translucens* var. *axillaris* (A.Br.) R.D.W. and *Chara corallina* Klein ex Willd., em. R.D.W. were grown in a substrate of soil, peat and sand in 10-50 litre aquaria filled with distilled water. The temperature was about 20° C and fluorescent lamps provided a 16/8h light/dark cycle. Non-elongating, mature internodal cells of the main axis or the branchlets were harvested 1 d prior to experiments, trimmed of neighbouring internodal cells and left overnight in artificial fresh water (10^{-3} M NaCl, 10^{-4} M KCl, 10^{-4} M $CaCl_2$).

Cells were wounded by 7-10 min irradiation with the HBO100 mercury lamp of a fluorescence microscope using a 63x microscope lens and a filter cube for GFP-fluorescence (450-490/510/515 nm) or by irradiation with a HBO50 mercury lamp in combination with a UV filter cube (365/395/420nm). Wound responses were also induced in the confocal laser scanning microscope (CLSM) by repeated scanning with the 375 nm laser diode at maximum intensity and a pixel time of 0.05 ms for about 5 min (Klima & Foissner, 2011). For chemically induced wounds, cells were treated with 50 mM $CaCl_2$ or by 10^{-4} M chlortetracycline (Sigma, Deisenhofen, Germany) (Foissner, 1990). Tungsten needles sharpened by repeated immersion into boiling potassium nitrate were used for puncturing.

In vivo staining and inhibitor treatments

Cells were pulse labeled for 10 min with 10 μM FM1-43 (N-(3-triethylammoniumpropyl)-4-(4-(dibutylamino)styryl)pyridinium dibromide; Invitrogen, Darmstadt, Germany), an endocytic marker, diluted from a 500 μM stock solution in distilled water. The acidotropic dye LysotrackerTred DND-99 (LTred; Invitrogen; 1 mM stock solution in dimethyl sulfoxide, DMSO) was used at 1 μM. Mitochondria were stained with a 1 μM solution of Mitotracker orange CMTMRos (Invitrogen; 1 mM stock solution in DMSO). The ER was visualized by 1 μM freshly prepared 3, 3′ dihexyloxacarbocyanine iodide ($DiOC_6$;

Invitrogen; 10 mM stock solution in DMSO). LTred, Mitotracker orange and $DiOC_6$ were applied for 30 min. LTred- and $DiOC_6$-stained cells were washed for 10 min in artificial fresh water before use, Mitotracker orange-labelled cells were washed up to 30 min in order to reduce unspecific cell wall staining.

Calcofluor white (Sigma; 0.1 %) and purified aniline blue (Biosupplies, Melbourne; 0.03 mg/ml) were used to identify cellulose and callose, respectively.

The actin cytoskeleton was stained by perfusion with 0.32 μM Alexa Fluor 488-phalloidin (Invitrogen, Eugene, Oregon; 6,6 μM stock solution in methanol) diluted in perfusion solution as described (Foissner, 2004). Microtubules were labeled by perfusion with 2μM Paclitaxel, Oregon Green 488 conjugate (Invitrogen, 1 mM stock solution in DMSO).

Cells were exposed to 50 μM dichlorobenzonitrile (Serva, Heidelberg, Germany) diluted from a 10 mM stock solution in ethanol. Inhibitors were applied 30 min before wounding and remained present in the medium during and after wounding.

All dyes and inhibitors were diluted with artificial fresh water. Controls containing the solvents only had no visible effect on cytoplasmic streaming, wound healing or internalization of dyes.

Immunofluorescence

The procedure for immunofluorescence of actin was as described in (Foissner *et al.*, 1996). Briefly, actin was labelled by monoclonal mouse anti-actin N350 (Amersham, Buckinghampshire, England) at a concentration of 1:100. The secondary antibody was an FITC-conjugated sheep anti-mouse IgM (Silenus, Victoria,Australia) used at 1:80.

Confocal scanning microscopy

The confocal laser scanning microscopes (CLSMs) used in this study were a Zeiss (Jena, Germany) LSM 510 coupled to an Axiovert inverted microscope and a Leica (Mannheim, Germany) TCS SP5 coupled to a DMI 6000B inverted microscope. Images were taken as described in (Schmoelzer *et al.*, 2011).

Images produced by the CLSM software were further processed with Adobe Photoshop (Adobe Systems) or Amira (Visage Imaging, Berlin, Germany). All images presented in this study are single sections unless otherwise stated.

Transmission electron microscopy and negative staining

Internodal cells of *N. flexilis* were chemically fixed with 2 % glutaraldehyde dissolved in 0.1 M phosphate buffer, pH 7, postfixed in 1 % OsO_4 (both from Sigma) and further processed as described (Foissner, 1988b).

Polysaccharides were localized according to Thiery's method (Plattner & Zingsheim, 1987). Sections of chemically fixed cells were mounted on formvar coated gold grids, oxidised in 1 % periodic acid, washed in distilled water, incubated in 0.2 % thiocarbohydrazide in 20 % acetic acid for 2-12 hours, washed in dilute acetic acid and distilled water, incubated in 1 % aqueous silver proteinate for 30 min, washed in distilled water and viewed without further staining. Silver proteinate was omitted on control sections.

Calcium was localized by fixation in 5 % glutaraldehyde containing 2 % potassium antimonate and postfixation in 1 % OsO_4 and 1.5 % potassium antimonate precipitation with antimonate as described in (Foissner, 1998).

For negative staining, internodal cells with UV-induced windows were fixed in 2 % glutaraldehyde dissolved in 0.1 M phosphate buffer, pH 7, postfixed in 1 % OsO_4 (both from Sigma). Cells were then cut into cylinders from which the cytoplasm was removed by careful sucking with a pipette. The cytoplasmic cylinder was opened flat with the aid of fine needles, transferred to a carbon coated formvar grid and stained with 1 % uranyl acetate. Sections or negatively stained samples were viewed in a Phillips EM 400 electron microscope (Eindhoven, The Netherlands) or in a Zeiss (Oberkochen, Germany) Leo electron microscope.

Field emission scanning electron microscopy

Internodal cells of *N. flexilis* treated with 50 mM $CaCl_2$ for 3-6 h were fixed in 1 % (v/v) glutaraldehyde dissolved in PEM buffer (25 mm PIPES [1,4-piperazinediethanesulfonic acid], 0.5 mm $MgSO_4$, 2.5 mm EGTA, pH 7.2) as described (Sugimoto *et al.*, 2000). After rinsing three times in PEM buffer, cells were cut into cylinders which were opened longitudinally with fine scissors or a razor blade. These cell fragments were either extracted in 1 % TritonX-100/PBS for 30 min or bleached in 0.1% (v/v) sodium hypochlorite for 40 min or boiled in acetic acid and nitric acid and distilled water (8:1:2) for 30 min . After thoroughly rinsing in distilled water, samples were osmicated in cold 0.5% (v/v) OsO_4 for 15 min, rinsed in distilled water, and dehydrated through a graded ethanol series (30%, 50%, 70%, 95%, and 100% three times, 15 min for each step). Specimens were critical point dried using CO_2, mounted on stubs with double-sided sticky carbon tape, inner surface facing upward, and coated with platinum at 2.4 mA for 195 s. Cell wall fine structure was examined on a Hitachi S4500 Field emission scanning electron microscope (FESEM; Hitachi, Tokyo, Japan).

Results

The unwounded internodal cell

A schematic longitudinal section through an internodal cell is shown in Fig. 1B which is based on numerous light and electron microscopical studies about characean algae. The cell wall contains cellulose microfibrils embedded in a matrix of pectins and hemicellulosic polysaccharides (Neville & Levy, 1984; Sorensen *et al.*, 2010, 2011). The cytoplasm consists of a cortical, stationary layer outside the endoplasm, which is well-known for its conspicuous unidirectional cytoplasmic streaming. The cortical layer is dominated by helically arranged chloroplast files. Cortical ER and cortical mitochondria (not shown) are sandwiched between the outer surface of the chloroplasts and the plasma membrane. Cortical actin filaments and microtubules are present along the plasma membrane and have an orientation that is predominantly transverse to the longitudinal axis in elongating internodes and random in non-elongating mature cells (Figs 1B and C; Wasteneys & Williamson, 1987). The endoplasm contains numerous Golgi and multivesicular bodies, mitochondria, peroxisomes and up to several thousand nuclei. Cytoplasmic streaming is generated through the interaction of myosin-coated cisternae of the inner ER and the subcortical actin filament bundles situated along the inner surface of the chloroplast files (Figs 1B and D; reviewed by Shimmen 2007). Depending on the species, solid carbohydrate/protein inclusions or crystals of organic material are found in the inner regions of the endoplasm or within the large, central vacuole. In the light, characean internodes display alternating bands of acid and alkaline pH (Fig. 1E), a property which is important for inducing local wound responses when cells are exposed to certain toxic chemicals (Foissner, 1989).

Local wounding of internodal cells triggers a series of reactions that is independent of the wound type and only the magnitude of injury determines the extent of the wound response.

In the following section we describe – in the order of severity - three morphologically different types of wound responses induced by UV light or chemicals and we compare these experimentally obtained data with the healing of wounds that occur in the natural environment of these algae. These wound responses appear to be highly conserved and are similar in all species investigated so far.

Cortical windows

The weakest morphologically detectable wound response in characean internodal cells is the irreversible detachment of the stationary, cortical chloroplasts (Fig. 2A). Such “windows” were first used by Kamitsubo to enable visualizing the subcortical actin bundles by DIC microscopy (Kamitsubo, 1972). A convenient way for producing chloroplast-free areas is spot-like irradiation with the UV-lamp of a fluorescence microscope for several minutes or with the laser light of a CLSM. The (at least partial) detachment of chloroplasts is also a prerequisite for the healing of more severe wounds, which is associated with exocytosis of organelles and can be induced by longer UV-irradiation or by chemicals (see below). The first visible sign of damage is the interruption of active endoplasmic mass streaming in the irradiated area, which is probably caused by local influx of external Ca^{2+} (Williamson & Ashley, 1982). This leads to an accumulation of cytoplasm in the upstream (endoplasm delivering) region of the wound, which then travels passively over the damaged area until it is drawn away at the unwounded downstream region. At the same time a rounding of the previously ovate chloroplasts can be observed. The chloroplast files in the irradiated area then detach from the cortex and perform undulating movements before they are released into the endoplasm together with their associated actin bundles. Vesicles sometimes accumulate in the window but rarely fuse with the cell membrane. Their saltatory movements correspond to the transient formation of a small and loose actin meshwork. After several hours, continuous actin filament bundles are regenerated by elongation of the bundles outside the window (Fig. 2B; (Williamson *et al.*, 1984, Williamson & Hurley, 1986). Their orientation reflects the previously passive endoplasmic flow in the injured area (Williamson *et al.*, 1984). In the window, a cortical actin filament meshwork is absent, suggesting that it has been recruited to actin bundles in the absence of chloroplasts (Foissner *et al.*, 1996). Full recovery is indicated by uninterrupted, active cytoplasmic streaming across the window (see trajectories of fast moving organelles in Figs 2C and D). The window remains free of chloroplasts but mitochondria occasionally contact the region near the plasma membrane and remain attached for seconds or minutes before they are released and carried away with the streaming endoplasm (Fig. 2C). The ER is divided into a mesh like cortical ER adjacent to the plasma membrane and fast moving inner ER tubes and cisternae as in control regions in spite of the absence of chloroplasts (Fig. 2D).

Cortical microtubules persist (Kriskovich & Richmond, 1988) or disappear from the irradiated area (Foissner & Wasteneys, 1999). In case of disappearance they regenerate approximately at the same time as the actin bundles. In small windows (with a diameter of up to 30 μm) the orientation of microtubules is random as in control unwounded regions. In larger windows cortical microtubules are aligned more or less parallel to the actin filament bundles although they are not in intimate contact with each other (Fig. 2A and B). Inhibitor experiments suggest that these surviving or regenerated microtubules are flow-aligned (Kriskovich & Richmond, 1988; Foissner & Wasteneys, 1999). Microtubule reorientation by hydrodynamic forces of actomyosin-driven cytoplasmic streaming has also been reported from leek epidermal cells (Sainsbury *et al.*, 2008). Conversely, actin filaments have been shown to be aligned along microtubules during recovery from drug-induced disassembly in epidermal cells of *Arabidopsis thaliana* (Sampathkumar *et al.*, 2011).

Fibrillar wound walls

A more severe type of wound response is observed when a wound wall (fibrillar or amorphous) becomes deposited in the cortical window. Fibrillar wound walls are morphologically and chemically similar to the normal cell walls and consist of cellulose microfibrils embedded in a matrix of pectins and hemicelluloses (Foissner, 1990; 1992; Sorensen *et al.*, 2010; 2011). They can be induced by treatment with 50 mM $CaCl_2$ in internodal cells of the genus *Nitella* but not in those of *Chara*. Wound walls induced by $CaCl_2$ or other chemicals (see below) appear preferentially at the alkaline bands that form to enable CO_2 uptake in adjacent acid bands where photosynthesis is more active (Bulychev *et al.*, 2001; Foissner, 1989). Inhibition of pH banding by photosynthesis inhibitors or dark treatment causes a uniform pH at the cell surface and immersion of internodes in wound-inducing chemicals then has either no effect when dissolved at low pH or induces wound wall deposition along the entire cell surface when applied at pH 8.5 or higher, which is lethal for the cells (Foissner, 1989).

The first stages of the wound response are the same as described above for cortical windows. New images presented in this study show that microtubules disassemble and chloroplasts detach from the cortex (Figs 3A and C) but that reorganization of the actin cytoskeleton is much more pronounced. Dense meshworks of randomly oriented actin filaments are present beneath wounds and in the cortical regions adjacent to wounds (Figs 3B and C). They support the saltatory movement of vesicles to and away from the wound. Many of the vesicles fuse with the plasma membrane and secrete their content (principally pectic polysaccharides) while their membrane delivers cellulose synthase complexes. EM images showed that excess plasma membrane is recycled from these wound sites via coated vesicles (Foissner, 1990). Here we illustrate that the plasma membrane beneath the forming and the mature wound wall is stained by FM-dyes also after pulse-labelling, i.e. when FM-dyes are no longer present in the medium while the wound wall is secreted (Figs 3D and E). Thus, the numerous FM1-43-fluorescent organelles in the wound cytoplasm not (only) represent early endosomes derived from the plasma membrane but also include FM1-43-stained vesicles which fuse with the plasma membrane. These may represent secretory vesicles to which the FM dye is redistributed like in growing pollen tubes (Parton *et al.*, 2011) or “recycling endosomes” representing later endocytic stages. FM1-43-labelled organelles are also involved in the regeneration of a continuous plasma membrane beneath amorphous wound walls (see below and Klima and Foissner 2011).

The morphology of the wound walls depends on the rate of the wound wall synthesis and this rate is dependent on the intensity of alkaline banding, which can be manipulated by light and the supply of bicarbonate (e.g. Lucas, 1975). Transmission electron microscopy and polarization microscopy have both indicated that quickly grown wound walls consist of groups of protuberances with concentric or helical orientation of cellulose microfibrils (Foissner, 1990). Here we present FESEM images showing that thick bundles of cellulose microfibrils wrap around each other consistently in a right-handed, three-dimensional helical pattern (“cone helix”; Figs 3F and G). The surface of slowly grown wound walls, by contrast, consists of smooth bulges and their cellulose microfibrils lack any preferred orientation (Fig. 3H). Wound walls formed in the presence of the cellulose synthesis inhibitor, dichlorobenzonitrile are also formed by exocytosis of vesicles linked with membrane recycling (Foissner, 1992) but, consistent with the failure to produce crystalline cellulose, they comprise a loose network of Golgi-synthesized pectic and hemicellulosic polysaccharides interwoven by a loose network of few cellulose microfibrils (Fig. 3I). Cellulose microfibrils with a random orientation typical of non-elongating cells are present at the regions of the cell on which the wound wall is built (Fig. 3J).

Microtubules and continuous actin bundles are regenerated after completion of the fibrillar wound wall formation, which lasts up to 24 hours. Regenerated microtubules are preferentially located in the clefts between the wound wall protuberances and far from the regenerated actin bundles (Foissner, 1990). Their orientation is mostly random. However, microtubules at the tip of slowly growing bulges are exposed the hydrodynamic shear forces exerted by endoplasmic flow and are parallel to the streaming direction (Foissner, 1990).

Amorphous wound walls

The most severe wound response, the deposition of amorphous wound walls, can be induced by treatment of cells with chemicals that have Ca^{2+}-ionophore-like properties, such as A 23187 and chlortetracycline. These wound walls form preferentially at the alkaline regions of cells and their size can be manipulated by the pH and the Ca^{2+} content of the medium (Foissner, 1988a; 1989; 1990). The dependency of wound wall deposition on an alkaline pH could also be demonstrated by local treatment with Sephadex beads soaked in wound-inducing chemicals. This causes deposition of wall material at the acid regions of the cells when the pH of the Sephadex-medium was adjusted to pH of 8.5 or higher (Foissner, 1991). The deposition of amorphous wound walls induced by local, prolonged UV irradiation is independent of the pH banding pattern (Klima & Foissner, 2011).

Microtubule depolymerisation and detachment of chloroplasts are the first signs of damage during amorphous wound wall formation. Local reorganization of the actin cytoskeleton is even more pronounced than observed beneath fibrillar wound walls. Huge meshworks of randomly oriented actin filaments are present beneath the plasma membrane, between the detaching chloroplasts and in the cortex of neighboured regions, where chloroplasts are still anchored (Fig. 4A). Numerous actin rings, spirals and polygons with diameters between 2 and 30 μm are seen in the relatively stagnant endoplasm beneath the wound (Fig. 4A, inset). They are often but not always associated with the surface of nuclei or the surface of detached chloroplasts. Secretory vesicles, identified by their size (up to 500 nm in diametre; Foissner, 1988a and b) and refractive properties in DIC, move along the actin filaments towards and away from the wound area and occasionally become immobilized at the cell periphery (Fig. 4B). The spreading of their content has been documented with video-enhanced microscopy (Foissner *et al.*, 1998). In addition, FM-stained organelles gather at the wound and are deposited together with their fluorescent membranes. Some of them are also stained by Lysotracker red indicating an acidic content (Fig. 4C). The third organelle known to be involved in the formation of the amorphous wound wall is the ER, which gathers at the wound and becomes deposited (Fig. 4D) along with the secretory and other vesicles. These ER cisternae are heavily loaded with calcium, as visualized by precipitation with antimonate (Fig. 4F) or staining with alizarin red (Foissner, 1998). ER deposition is thus responsible for the high calcium content of the amorphous wound walls, which is also evident from the intense chlortetracycline-fluorescence (Foissner, 1988a) indicating membrane-bound calcium (Fig. 4E; Caswell & Hutchison, 1971; Schneider *et al.* 1983). The deposition of amorphous wound walls is associated with pronounced ion fluxes. Ca^{2+} disappears from the medium and the membrane potential becomes more positive (Foissner, 1989; Homblé & Foissner, 1993).

The secretion of secretory vesicles, putative endosomes and ER cisternae takes place without membrane recycling (“compound exocytosis”; Pickett & Edwardson, 2006). Crystalline cellulose is absent from the amorphous wound walls. Present instead is callose, a polysaccharide that is neither found in fibrillar wound walls nor in the normal cell wall (Foissner, 1989, 1992). The end of wound healing, after less than one hour of chemical exposure, is indicated by a continuous plasma membrane (Fig. 4G) which is probably formed by the fusion of secretory vesicles and putative endosomes (Klima & Foissner, 2011), as described above for fibrillar wound walls. Excess membrane is then recycled via

coated pits and coated vesicles and, eventually, a thin fibrillar wound wall is deposited. Finally, continuous actin bundles are regenerated over the wound. Amorphous wound walls have a flat, smooth surface. Regenerated microtubules are thus mostly exposed to endoplasmic flow and aligned parallel to the streaming direction (not shown).

Wound walls induced by mechanical damage, pathogens and alkaline banding

In their natural environment, characean internodes are exposed to mechanical damage by water currents and animals, which cause bending, often culminating in rupture of the cell wall. Cell wall holes are sealed by conspicuous solid inclusions which are expelled automatically due to the turgor of the cell (Figs 5A-C). These solid inclusions, called "echinate bodies" in the genus *Nitella* because of their fuzzy surface, form within membrane-bound compartments located at the inner regions of the streaming endoplasm and, depending on the species, are eventually delivered to the large central vacuole (Fig. 1B). They consist of polysaccharides covered by a protein layer which appears to glue the solid inclusions with each other and with the cell wall (Foissner, 1988b). Onto this external, passively formed wound plug, a bipartite wound wall is actively deposited (Klima & Foissner, 2011). The outer layer resembles the amorphous wound wall in formation, morphology and chemistry (Fig. 5B-E). It consists of the contents and membranes of secretory and FM-stained organelles (Figs 5 B and E) and of cisternae of the ER (Fig. 5 D) and contains callose (Fig. 5G). The inner, membrane-free layer has the characteristics of the fibrillar wound wall and consists of cellulose microfibrils embedded in a pectin-rich matrix (Fig. 5F).

Local, fibrillar or amorphous wound walls or a combination of both are found beneath invading fungal hyphae and beneath bacteria, which colonize and degrade the primary and, occasionally, also the secondary walls of older cells (Fig. 5H).

Finally, deposition of fibrillar wound walls with a diameter of up to 20 μm can often be observed at the alkaline regions of cells exposed to high light intensities (Fig. 5I). In old, degenerating internodes fibrillar wound walls are distributed over the whole surface.

Discussion

The characean internodal cell as a model system for studying wound responses

Characean internodal cells readily react to wounding and show different types of wound responses. The morphological and physiological criteria used for their classification are summarized in Table 1 and reflect the extent of damage and the severity of the response. Accordingly, we distinguish between cortical window formation (detachment of chloroplasts in the absence of wound wall deposition), the formation of fibrillar wound walls (exocytosis of vesicles coupled with membrane recycling, a process similar to the formation of the normal cell wall) and the deposition of amorphous wound walls (exocytosis of vesicles and ER cisternae without membrane recycling). The property of internodes to react differently but reproducibly to damage caused by chemicals, light or puncturing make the characean internodal cell a useful model system for studying various aspects of wound healing, as well as rapid cell wall growth, such as that occurring during tip growth e.g. (Krichevsky *et al.*, 2007) or the formation of wall ingrowths in transfer cells (Offler *et al.*, 2003).

An increase in cytosolic Ca^{2+} concentration determines the extent of the wound response

The available data (type of wound induction and response of the cell) suggest that a rise in cytosolic free Ca^{2+} coming either from internal stores (Thiel *et al.*, 2003) and/or from the apoplast or the medium determines the extent of wounding and the response of the cell. It has long been known that a sudden increase in cytosolic free Ca^{2+} stops cytoplasmic

streaming in characean internodal cells (Williamson & Ashley, 1982), is involved in the organization of the actin cytoskeleton (e.g. Zhang *et al.*, 2011), in the induction of exocytosis (Thiel *et al.*, 1995), in callose synthesis (Luna *et al.*, 2011) and in mediating the plant's response to wounding (Dombrowski & Bergey, 2007). We therefore hypothesize that a small Ca^{2+} influx (or release from internal stores) causes the arrest of cytoplasmic streaming and the detachment of chloroplasts (window formation; Fig. 6A and B). A moderate influx of Ca^{2+} can be induced by high $CaCl_2$ concentration in the medium and, in addition to the changes described above, this leads to a reorganization of the actin cytoskeleton and to exocytosis of vesicles coupled with membrane recycling (deposition of a fibrillar wound wall; Fig. 6C). During high Ca^{2+} influx caused by treatment with ionophores, vesicles fuse not only with the plasma membrane but also with cisternae of the ER in the absence of membrane recycling (deposition of an amorphous wound wall; Fig. 6D). The ER cisternae are heavily loaded with calcium and their deposition into the extracytoplasmic space could be an efficient emergency reaction to Ca^{2+} overload (Foissner, 1998).

In their natural environment characean algae are wounded mechanically or by pathogens. The wound walls are often bilayered, with an outer layer having the characteristics of an amorphous wound wall and an inner, fibrillar layer (Klima & Foissner, 2011 and this study). The outer, amorphous wound wall is probably used for Ca^{2+} seclusion and rapid sealing by callose whereas the inner, fibrillar wound wall confers mechanical stability. We show also that high photosynthetic activity in characean internodes is often correlated with wound responses at the alkaline bands of cells indicating enhanced Ca^{2+} fluxes over the plasma membrane in these regions. The benefit of increased carbon assimilation in acid bands comes at the cost of an enhanced "weakness" of the plasma membrane at the alkaline regions.

Putative endosomes involved in membrane repair

It has previously been shown that – in addition to secretory vesicles and ER-cisternae - FM-stained organelles accumulate and are deposited in the periphery of cells irradiated locally with 375 nm at high laser intensity (Klima & Foissner, 2011). These organelles deliver the FM-fluorescence of regenerated, continuous plasma membrane and thus appear to be involved in plasma membrane repair during formation of amorphous wound walls. New images presented in this study show an FM-fluorescent plasma membrane beneath fibrillar wound walls although cells were pulse-labelled before treatment. This suggests that the numerous FM-fluorescent organelles at fibrillar wounds represent not only organelles involved in membrane retrieval but also organelles involved in membrane delivery. Recent data indicate that these "secretory or recycling endosomes" carry the Rab GTPase ARA6 supposed to be an endosomal marker in *Arabidopsis thaliana* (Ebine & Ueda, 2009). FM-fluorescence recycling has also been suggested for unwounded cells because, in contrast to the plasma membrane of higher plants, the plasma membrane of characean internodes remains stained for at least 24 hours after pulse labelling (Klima & Foissner, 2008).

That there is no general delivery of organelles towards the wound is evident from the behaviour of nuclei and mitochondria, which are excluded from and – in the case of mitochondria - even appear to escape the wound cytoplasm when the amorphous wound wall is deposited (Klima & Foissner, 2011).

The cytoskeleton plays a pivotal role in the wound response

Local wounding destroys existing cellular polarities and establishes new ones. In cells without inherent polarity like the diffusely elongating internodal cells, local wounding induces transient changes in cytoarchitecture, which is reminiscent of tip-growing cells such

as pollen tubes or root hairs in which cell wall-forming organelles are transported to the growing end (Higaki *et al.*, 2011). These changes in cytoarchitecture are mainly due to reorganization of the actin cytoskeleton, which provides the tracks for targeted delivery of wall forming organelles. In this article we show that the extent of the wound response, which is apparently correlated with the extent of Ca^{2+} influx, is also correlated with the degree of actin reorganization. Especially notable is the formation of numerous actin rings at the highest stress intensity, i.e. during the deposition of amorphous wound walls. Actin rings are occasionally observed in unwounded characean and other cells (e.g. Chaidee *et al.*, 2008; Smertenko *et al.*, 2010). The number of actin rings in tobacco BY-2 cells could be significantly reduced by omitting the growth regulator auxin from the medium and it has been suggested that actin rings represent a storage form for surplus actin (Smertenko *et al.*, 2010). In cells of *Chenopodium rubrum,* the number of actin rings increases significantly when suspension cultures are exposed to heat shock at a temperature of 41° C, which is correlated with specific ion fluxes (Chaidee *et al.*, 2008). This could indicate that the formation of actin rings is involved in stress sensing or stress response or, at least, reflects a specific status of the cytoplasm.

Microtubules are not required for wound wall deposition but their disassembly is one of the earliest detectable signs of damage. This could, in combination with other factors, be an important signal for early stages of wound responses. In unwounded internodal cells, depolymerisation of microtubules enhances reversible, cytochalasin-dependent reorganization of the actin cytoskeleton (Foissner & Wasteneys, 2000b). A possible scenario is that the formation of an actin meshwork beneath wounds is aided by the release of a microtubule-associated protein (discussed in Foissner & Wasteneys, 2000b; compare Deeks *et al.*, 2010). In wheat, microtubules have been described to be involved in sensing low temperature stress and their disassembly has been assumed to be a trigger for cold acclimation (Abdrakhamanova *et al.*, 2003). In *Arabidopsis*, adaptation to salt stress requires microtubule disassembly (Wang *et al.*, 2007).

Ordered deposition of cellulose microfibrils in the absence of microtubules

The exact role of microtubules in the ordered deposition of cellulose microfibrils is still a matter of dispute. On the one hand, cortical microtubules interact with cellulose synthase (CESA) trafficking compartments and appear to affect their positioning at the plasma membrane (Gutierrez *et al.*, 2009). On the other hand, CESA complexes have been reported in the absence of microtubules to move in parallel order at oblique angles to the cell axis (Paradez *et al.*, 2006) and highly ordered transverse orientations of cellulose microfibrils have been observed in the *Arabidopsis* microtubule mutant *mor1-1* (Sugimoto *et al.*, 2003). The FESEM images of fibrillar wound walls revealed a helical arrangement of cellulose microfibrils. These findings confirm that the highly structured cell walls produced do not require microtubules for their deposition or for their complex morphology. They indicate, however, that a critical rate of cellulose synthesis is necessary for the presumed self-assembly of cellulose microfibrils into helical aggregates (compare Mulder *et al.*, 2004; Emons *et al.*, 2007). A possible scenario is that activated cellulose synthase complexes default to new helical trajectories that respond to and assist the deposition of membrane indentations. This altered behaviour could be driven by membrane heterogeneities, which have been suggested to play a role in altering cellulose crystallinity in *Arabidopsis* (Fujita *et al.*, 2011). Radial Ca^{2+} diffusion gradients could also “trap” synthase complexes into helical trajectories so that they are forced to deposit cellulose microfibrils towards the interior of the cell.

Acknowledgments

This research was funded by the Austrian Science Fund (FWF): project no. P 22957-B20 and the Australian Research Council.

Abbreviations

CESA	cellulose synthase
CLSM	confocal laser scanning microscope
DIC	differential interference contrast
$DiOC_6$	3, 3′ dihexyloxacarbocyanine iodide
DMSO	dimethyl sulfoxide
ER	endoplasmic reticulum
FESEM	field emission scanning electron microscope

References

Abdrakhamanova A, Wang QY, Khokhlova L, Nick P. Is microtubule disassembly a trigger for cold acclimation? Plant Cell Physiol. 2003; 44:676–686. [PubMed: 12881495]

Braun M, Foissner I, Lühring H, Schubert H, Thiel G. Characean algae: Still a valid model system to examine fundamental principles in plants. Prog. Bot. 2007; 68:193–220.

Bulychev AA, Cherkashin AA, Rubin AB, Vredenberg WJ, Zykov VS, Mueller SC. Comparative study on photosynthetic activity of chloroplasts in acid and alkaline zones of *Chara corallina*. Bioelectrochemistry. 2001; 53:225–232. [PubMed: 11339311]

Caswell AH, Hutchison JD. Visualization of membrane bound cations by a fluorescent technique. Biochem. Biophys. Res. Comm. 1971; 42:43–49. [PubMed: 5546350]

Chaidee A, Foissner I, Pfeiffer W. Cell-specific association of heat shock-induced proton flux with actin ring formation in *Chenopodium* cells: comparison of auto- and heterotroph cultures. Protoplasma. 2008; 234:33–50. [PubMed: 18807117]

Deeks MJ, Fendrych M, Smertenko A, Bell KS, Oparka K, Cvrckova F, Zarsky V, Hussey PJ. The plant formin AtFH4 interacts with both actin and microtubules, and contains a newly identified microtubule-binding domain. J. Cell Sci. 2010; 123:1209–1215. [PubMed: 20332108]

Dombrowski JE, Bergey DR. Calcium ions enhance systemin activity and play an integral role in the wound response. Plant Science. 2007; 172:335–344.

Ebine K, Ueda T. Unique mechanism of plant endocytic/vacuolar transport pathways. J. Plant Res. 2009; 122:21–30. [PubMed: 19082690]

Emons AMC, Höfte H, Mulder BM. Microtubules and cellulose microfibrils: how intimate is their relationship? Trends Plant Sci. 2007; 12:279–281. [PubMed: 17591457]

Foissner I. Chlortetracycline-induced formation of wall appositions (callose plugs) in internodal cells of *Nitella flexilis* (Characeae). J. Phycol. 1988a; 24:458–467.

Foissner I. The relationship of echinate inclusions and coated vesicles on wound-healing in *Nitella flexilis* (Characeae). Protoplasma. 1988b; 142:164–175.

Foissner I. pH-dependence of chlortetracycline-induced plug formation in *Nitella flexilis* (Characeae). J. Phycol. 1989; 25:313–318.

Foissner I. Wall appositions induced by ionophore A 23187, CaCl2, LaCl3, and nifedipine in characean cells. Protoplasma. 1990; 154:80–90.

Foissner I. Induction of exocytosis in characean internodal cells by locally restricted application of chlortetracycline and the effect of cytochalasin B, depolarizing and hyperpolarizing agents. Plant, Cell Environm. 1991; 14:907–915.

Foissner I. Effects of dichlorobenzonitrile on the formation of cell wall appositions (plugs) in internodal cells of *Chara corallina* Klein ex. Willd, em. R.D.W. and *Nitella flexilis* (L.) Ag. New Phytol. 1992; 121:447–455.

Foissner I. Localization of calcium ions in wounded characean internodal cells. New Phytol. 1998; 139:449–458.

Foissner I. Microfilaments and microtubules control the shape, motility, and subcellular distribution of cortical mitochondria in characean internodal cells. Protoplasma. 2004; 224:145–157. [PubMed: 15614475]

Foissner I, Lichtscheidl IK, Wasteneys GO. Actin-based vesicle dynamics and exocytosis during wound wall formation. Cell Motil. Cytoskeleton. 1996; 35:35–48. [PubMed: 8874964]

Foissner I, Lichtscheidl IK, Wasteneys GO. Actin-based vesicle dynamics and exocytosis during wound wall formation. Video supplement. Cell Motil. Cytoskeleton. 1998; 39:346–347. [PubMed: 9556338]

Foissner I, Wasteneys GO. Microtubules at wound sites of *Nitella* internodal cells passively co-align with actin bundles when exposed to hydrodynamic forces generated by cytoplasmic streaming. Planta. 1999; 208:480–490.

Foissner, I.; Wasteneys, GO. Actin in characean internodal cells. In: Staiger, C.; Baluska, DF.; Volkmann, D.; Barlow, P., editors. Actin: A dynamic framework for multiple plant cell functions. Kluwer Academic Publisher; Dordrecht, Boston, London: 2000a. p. 259-274.

Foissner I, Wasteneys GO. Microtubule disassembly enhances reversible cytochalasin-dependent disruption of actin bundles in characean internodes. Protoplasma. 2000b; 214:33–44.

Gutierrez R, Lindeboom JJ, Paredez AR, Emons AMC, Ehrhardt DW. *Arabidopsis* cortical microtubules position cellulose synthase delivery to the plasma membrane and interact with cellulose synthase trafficking compartments. Nat. Cell Biol. 2009; 11:797–806. [PubMed: 19525940]

Hardham AR, Jones DA, Takemoto D. Cytoskeleton and cell wall function in penetration resistance. Curr. Opin. Plant Biol. 2007; 10:342–348. [PubMed: 17627866]

Higaki T, Kurusu T, Hasezawa S, Kuchitsu K. Dynamic intracellular reorganization of cytoskeletons and the vacuole in defense responses and hypersensitive cell death in plants. J. Plant Res. 2011; 124:315–324. [PubMed: 21409543]

Homblé F, Foissner I. Electron microscopy and electrophysiology of local cell wall formation in *Chara corallina*. Plant Cell Physiol. 1993; 34:1283–1289.

Kamitsubo E. A “window technique” for detailed observation of characean cytoplasmic streaming. Exp. Cell Res. 1972; 74:613–616. [PubMed: 5080800]

Klima A, Foissner I. FM dyes label sterol-rich plasma membrane domains and are internalized independently of the cytoskeleton in characean internodal cells. Plant Cell Physiol. 2008; 49:1508–1521. [PubMed: 18757863]

Klima A, Foissner I. Actin-dependent deposition of putative endosomes and endoplasmic reticulum during early stages of wound healing in characean internodal cells. Plant Biol. 2011; 13:590–601. [PubMed: 21668600]

Krichevsky A, Kozlovsky SV, Tian GW, Chen MH, Zaltsman A, Citovsky V. How pollen tubes grow. Dev. Biol. 2007; 303:405–420. [PubMed: 17214979]

Kriskovich MD, Richmond PA. Flow-alignment of microtubules in *Nitella*. J. Cell Biol. 1988; 107(144):29a.

Lucas WJ. The influence of light intensity on the activation and operation of the hydroxyl efflux system of *Chara corallina*. J. Exp. Bot. 1975; 26:347–360.

Luna E, Pastor V, Robert J, Flors V, Mauch-Mani B, Ton J. Callose deposition: a multifaceted plant defense response. Mol. Plant-Microbe Interact. 2011; 24:183–193. [PubMed: 20955078]

Menzel D. How do giant plant cells cope with injury?-The wound response in siphonous green algae. Protoplasma. 1988; 144:73–91.

Mulder B, Schel J, Emons AM. How the geometrical model for plant cell wall formation enables the production of a random texture. Cellulose. 2004; 11:395–401.

Nagai R. Regulation of intracellular movements in plant cells by environmental stimuli. Int. Rev. Cytol. 1993; 145:251–310.

Neville AC, Levy S. Helicoidal orientation of cellulose microfibrils in *Nitella opaca* internode cells ultrastructure and computed theoretical effects of strain reorientation during wall growth. Protoplasma. 1984; 162:370–384.

Offler CE, McCurdy DW, Patrick JW, Talbot MJ. Transfer cells: Cells specialized for a special purpose. Annu. Rev. Plant Biol. 2003; 54:431–454. [PubMed: 14502998]

Paradez A, Wright A, Ehrhardt DW. Microtubule cortical array organization and plant cell morphogenesis. Curr. Opin. Plant Biol. 2006; 9:571–578. [PubMed: 17010658]

Parton RM, Fischer-Parton S, Watahiki MK, Trewavas AJ. Dynamics of the apical vesicle accumulation and the rate of growth are related in indivudual pollen tubes. J. Cell Sci. 2001; 114:2685–2695. [PubMed: 11683395]

Pickett JA, Edwardson JM. Compound exocytosis: Mechanisms and functional significance. Traffic. 2006; 7:109–116. [PubMed: 16420520]

Plattner, H.; Zingsheim, H-P. Elektronenmikroskopische Methodik in der Zell- und Molekularbiologie. Fischer; Stuttgart: 1987.

Proseus TE, Boyer JS. Periplasm turgor pressure controls wall deposition and assembly in growing *Chara corallina* cells. Ann. Bot. (Lond). 2006; 98:93–105.

Qiu YL. Phylogeny and evolution of charophytic algae and land plants. J. Syst. Evol. 2008; 46:287–306.

Sainsbury F, Collings DA, Mackun K, Gardiner J, Harper JDI, Marc J. Developmental reorientation of transverse cortical microtubules to longitudinal directions: a role for actomyosin-based streaming and partial microtubule-membrane detachment. Plant J. 2008; 56:116–131. [PubMed: 18557839]

Sampathkumar A, Lindeboom JJ, Debolt S, Gutierrez R, Ehrhardt DW, Ketelaar T, Persson S. Live cell imaging reveals structural associations between the actin and microtubule cytoskeleton in *Arabidopsis*. Plant Cell. 2011; 23:2302–2313. [PubMed: 21693695]

Schmoelzer PM, Höftberger M, Foissner I. Plasma membrane domains participate in pH-banding of *Chara* internodal cells. Plant Cell Physiol. 2011; 52:1274–1288. [PubMed: 21659328]

Schneider AS, Herz R, Sonenberg M. Chlortetracycline as a probe of membrane-associated calcium and magnesium: Interaction with red cell membranes, phospholipids, and proteins monitored by fluorescence and circular dichroism. Biochemistry. 1983; 22:1680–1686. [PubMed: 6849877]

Shimmen T. The sliding theory of cytoplasmic streaming: fifty years of progress. J. Plant Res. 2007; 120:31–43. [PubMed: 17252175]

Shimmen T. Electrophysiological characterization of the node in *Chara corallina*: Functional differentiation for wounding response. Plant Cell Physiol. 2008; 49:264–272. [PubMed: 18182401]

Smertenko AP, Deeks MJ, Hussey PJ. Strategies of actin reorganisation in plant cells. J. Cell Sci. 2010; 123:3019–3028. [PubMed: 20699356]

Sorensen I, Domozych D, Willats WGT. How have plant cell walls evolved? Plant Physiol. 2010; 153:366–372. [PubMed: 20431088]

Sorensen I, Pettolino FA, Bacic A, Ralph J, Lu F, O'Neill MA, Fei Z, Rose JKC, Domozych DS, Willats WGT. The charophycean green algae provide insights into the early origins of plant cell walls. Plant J. 2011 (in press).

Sugimoto K, Himmelspach R, Williamson RE, Wasteneys GO. Mutation or drug-dependent microtubule disruption causes radial swelling without altering parallel cellulose microfibril deposition in *Arabidopsis* root cells. Plant Cell. 2003; 15:1414–1429. [PubMed: 12782733]

Sugimoto K, Williamson RE, Wasteneys GO. New techniques enable comparative analysis of microtubule orientation, wall texture, and growth rate in intact roots of *Arabidopsis*. Plant Physiol. 2000; 124:1493–1506. [PubMed: 11115865]

Tazawa M, Shimmen T. How characean cells have contributed to the progress of plant membrane biophysics. Aust. J. Plant Physiol. 2001; 28:523–539.

Thiel G, Rupnik M, Zorec R. Raising the cytosolic Ca^{2+} concentration increases the membrane capacitance of maize coleoptile protoplasts: Evidence for Ca^{2+}-stimulated exocytosis. Planta. 1995; 195:305–30827.

Thiel G, Wacke M, Foissner I. Ca^{2+} mobilization from internal stores in electrical membrane excitation in *Chara*. Prog. Bot. 2003; 64:217–233.

Wang C, Li J, Yuan M. Salt tolerance requires cortical microtubule reorganization in *Arabidopsis*. Plant & Cell Physiol. 2007; 48:1534–1547. [PubMed: 17906320]

Wasteneys GO, Williamson RE. Microtubule orientation in developing internodal cells of *Nitella*: a quantitative analysis. Eur. J. Cell Biol. 1987; 43:14–22.

Wasteneys GO, Williamson RE. Reassembly of microtubules in *Nitella tasmanica* - assembly of cortical microtubules in branching clusters and its relevance to steady-state microtubule assembly. J. Cell Sci. 1989; 93:705–714.

Wei CF, Lintilhac PM. Loss of stability: A new look at the physics of cell wall behavior during plant cell growth. Plant Physiol. 2007; 145:763–772. [PubMed: 17905864]

Williamson RE, Ashley CC. Free Ca^{2+} and cytoplasmic streaming in the alga *Chara*. Nature. 1982; 296:647–651. [PubMed: 7070508]

Williamson, RE.; Grolig, F.; Hurley, UA.; Jablonski, PP.; Mccurdy, DW.; Wasteneys, GO. Methods for studying the plant cytoskeleton. In: Linskens, HF.; Jackson, JF., editors. Modern methods of plant analysis N.S., vol 10 Plant fibers. Springer; Berlin: 1989. p. 203-218.

Williamson RE, Hurley UA. Growth and regrowth of actin bundles in *Chara* - bundle assembly by mechanisms differing in sensitivity to cytochalasin. J. Cell Sci. 1986; 85:21–32. [PubMed: 3793793]

Williamson RE, Hurley UA, Perkin JL. Regeneration of actin bundles in *Chara*: polarized growth and orientation by endoplasmic flow. Eur. J. Cell Biol. 1984; 34:221–228. [PubMed: 6479173]

Zhang Y, Xiao YY, Du F, Cao LJ, Dong HJ, Ren H. *Arabidopsis* VILLIN4 is involved in root hair growth through regulating actin organization in a Ca^{2+}-dependent manner. New Phytol. 2011; 190:667–682. [PubMed: 21275995]

Europe PMC Funders Author Manuscripts

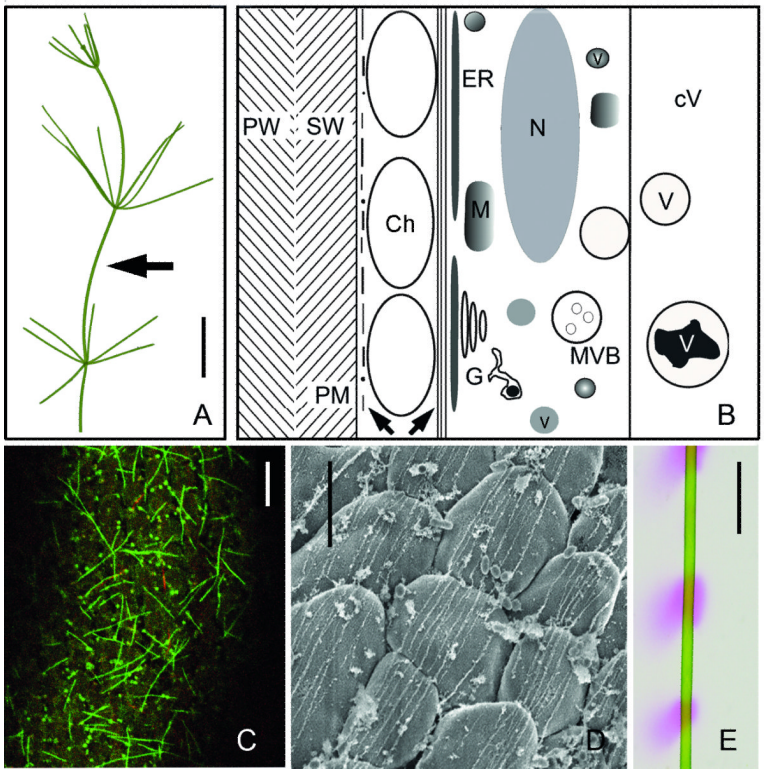

Fig. 1.

Characean internodal cell organization and pH banding. (A) A thallus of *Nitella translucens*. Arrow indicates an internodal cell from the main axis. (B) Schematic representation of the cytoarchitecture of an internodal cell (longitudinal section), drawn approximately to scale. Left arrow indicates cortical actin filaments and microtubules, right arrow points to the subcortical actin filament bundles. Ch = chloroplast, cV = central vacuole, G = Golgi body, ER = endoplasmic reticulum, M = mitochondrion, MVB = multivesicular body, N = nucleus, PM = plasma membrane, PW = primary wall, SW = secondary wall, v = vesicle, V = subvacuole. (C) Cortical microtubules (green) and actin filaments (red) in an internodal cell of *N. translucens* stained by perfusion with fluorescent taxol and fluorescent phalloidin. (D) High resolution SEM image of subcortical actin bundles located at the inner surface of chloroplast files (*N. flexilis;* Triton-extracted). (E) pH banding pattern of an internodal cell of *N. translucens* visualized by phenol red. Pink regions indicate regions of net H^+ influx, which generates an extracellular alkaline pH. Bars are 1 cm (A, E), 10 μm (C) and 5 μm (D)

Europe PMC Funders Author Manuscripts

Europe PMC Funders Author Manuscripts

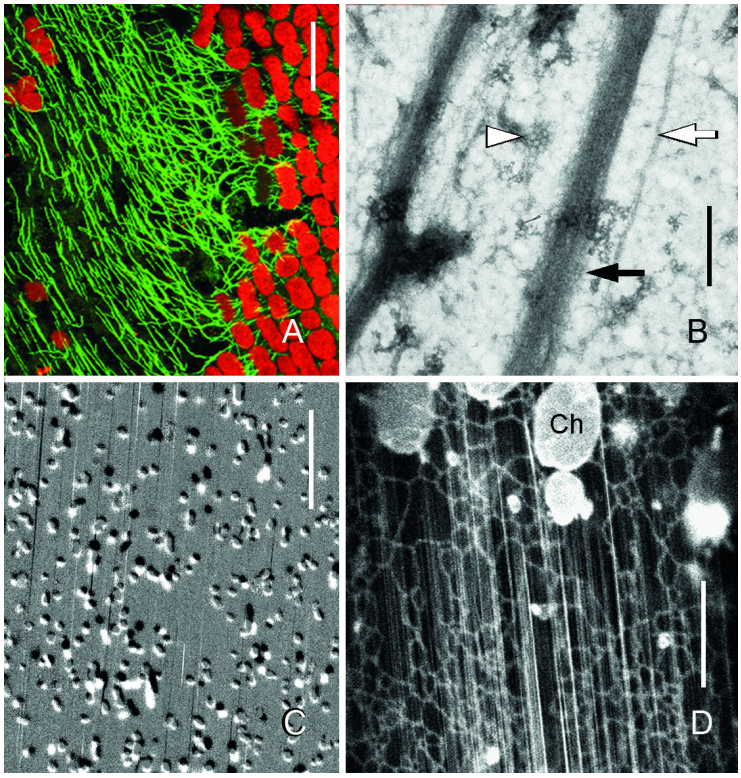

Fig. 2.

"Healed" windows induced by local irradiation with UV of internodal cells of *Nitella flexilis*. (A) Regenerated microtubules (green) visualized by immunofluorescence. Note how orientation of many microtubules is parallel to the autofluorescent chloroplast files (red) in the window and transverse to the files in the neighbouring unwounded region. (B) Negative stain preparation of the cortex. Black arrow indicates an actin filament bundle, white arrow indicates a microtubule. Arrow head indicates a coated pit. (C) Cortical mitochondria. Two images were taken at 75 sec intervals and subtracted from each other in order to show displacement. Most mitochondria were immobile and appear grey; moving organelles are black and white, respectively. Streaks are trajectories of fast organelles in the endoplasm. (D) $DiOC_6$-stained mesh-like cortical ER and subcortical ER tubes (streaks) in the endoplasm. Ch = chloroplast at the border of the window. Bars are 400 nm (B), 10 μm (C and D) and 20 μm (A).

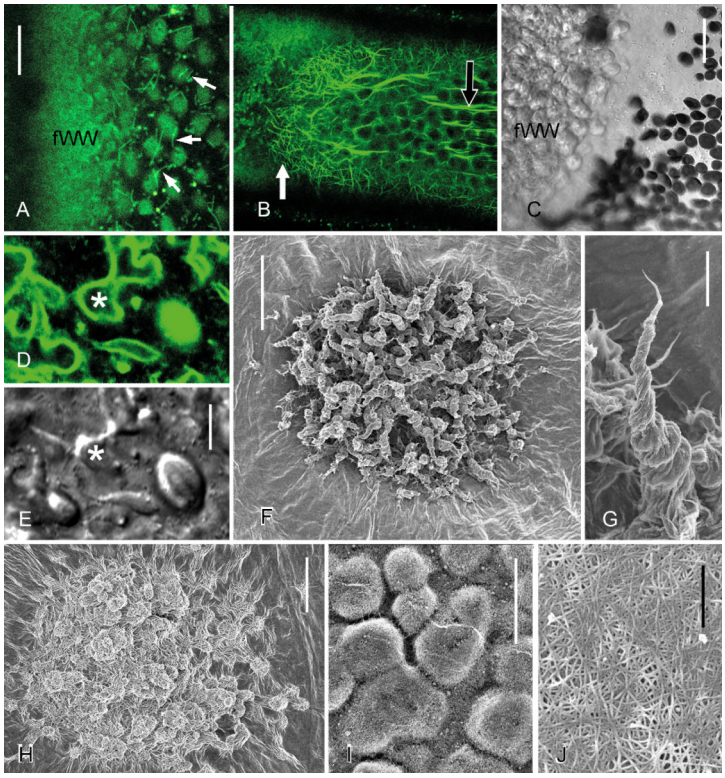

Fig. 3.

Fibrillar wound walls induced by treatment of internodal cells of *Nitella flexilis* with 50 mM $CaCl_2$. Images were taken after 2 h (A, D, E), 6 h (B, C, F, G, I) and 24 h (H) treatment. (A) Microtubules are absent where a fibrillar wound wall (fWW) is deposited. Short microtubules visualized by perfusion of fluorescent taxol (arrows) are present near the wound (compare with Fig. 1C). (B and C) A dense meshwork of actin filaments stained by perfusion with fluorescent phalloidin is present during the deposition of a fibrillar wound (white arrow in B). The black arrow indicates a subcortical actin bundle. The DIC image C corresponds to the left side of image B. (D and E) FM1-43-stained plasma membrane and organelles (D) at protuberances (*) of a forming fibrillar wound wall. E is the corresponding DIC image. (F and G) Quickly formed fibrillar wound walls consisting of groups of protuberances (F) in which cellulose microfibrils wrap around each other to form a right-handed helix (G). (H) Slowly formed fibrillar wound wall in which protuberances lack helical shape. (I) Wound wall grown in the presence of a cellulose synthesis inhibitor (50 μM DCB dissolved in 50 mM $CaCl_2$). (J) Cellulose microfibril orientation in the secondary cell wall onto which the wound walls are deposited. F-J are FESEM images of the inner surface of wound walls and cell walls, respectively, and obtained after hypochlorite extraction of cytoplasm and membrane content (F-I) or after acid treatment (I). Bars are 500 nm (J), 2 μm (G), 5 μm (D and E), 10 μm (A and I) and 20 μm (B and C, F, H)

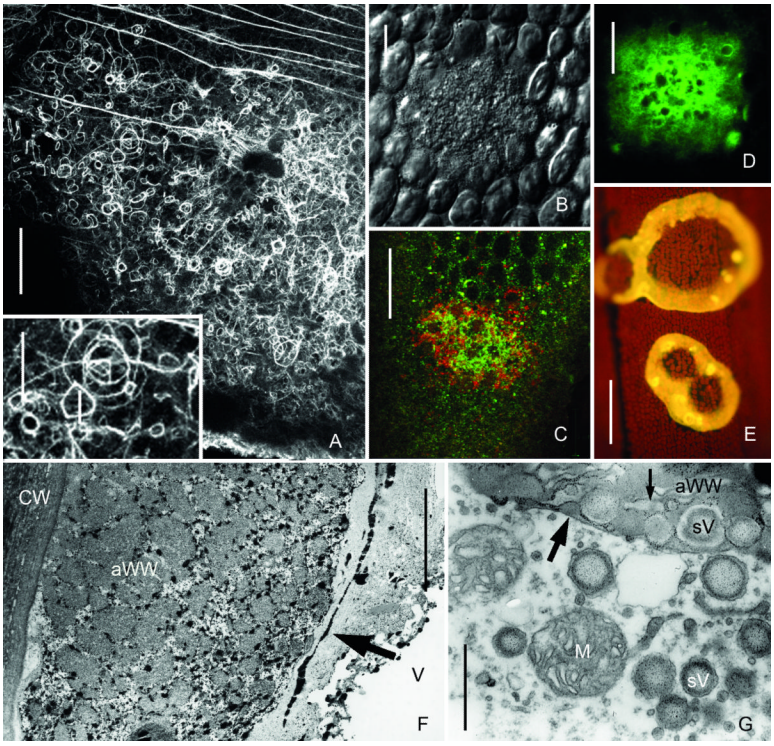

Fig. 4.

Amorphous wound walls induced by treatment of internodal cells of *Nitella flexilis* with 10^{-4} M chlortetracycline for one hour (A, F and G) and by 2 min local irradiation with UV of internodal cells of *Chara corallina* (B-E). (A) Actin cytoskeleton beneath a forming amorphous wound wall visualized by immunofluorescence. Note numerous actin rings and polygons (inset). Continuous actin bundles are present outside the wound. (B-D) Accumulation of secretory vesicles (B) and of FM1-43- (green) and Lysotracker red-stained organelles (C) and of $DiOC_6$-stained ER (D) in UV-irradiated areas. (E) The yellow chlortetracycline-fluorescence of the wound walls indicates membrane-bound calcium. (F-G) TEM images of amorphous wounds. Black antimonite deposits in F indicate high calcium concentrations in the amorphous wound wall (aWW) and in the ER cisternae (arrow in F). Faint granules in G indicate polysaccharides visualized by the Thiery method. Note remnants of secretory vesicles (sV) and ER (small arrow) in the amorphous wound wall, which is already covered by a continuous plasma membrane (large arrow). Bars are 1 μm (G), 5 μm (F), 10 μm (B-E), 20 μm (inset in A) and 50 μm (A)

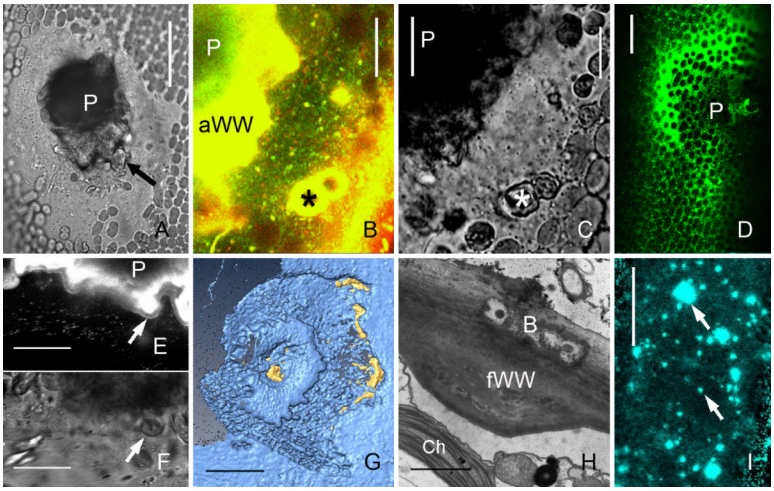

Fig. 5.

Wound walls induced by mechanical damage (puncturing), by bacteria and wound walls at alkaline regions of a cell exposed to high light intensity. (A-G) Puncture wounds in internodal cells of *Chara corallina*. (A) Bright field image of a healed wound. A fibrillar wound wall (arrow) is seen around the wound plug (P). (B and C) FM1-43 (green) and Lysotracker red-stained organelles are deposited near the wound plug (P) and around damaged chloroplasts (*) in early stages of wound healing (15 min after puncturing). C is the corresponding bright field image. (D) $DiOC_6$-stained ER deposited at a wound 30 min after puncturing. (E and F) Wound plug (P) and FM1-43-fluorescent amorphous wound wall of a healed wound. A continuous FM1-43-fluorescent plasma membrane (arrow) is seen along the non-fluorescent inner, fibrillar wound wall 60 min after puncturing). F is the corresponding bright field image. (G) 3-D reconstruction of the inner surface of a healed puncture wound showing parts of the callose containing outer wound wall stained by aniline blue (yellow) and the calcofluor-labelled inner cellulosic wound wall (cyan), which is continuous with the normal cell wall. (H) Fibrillar wound wall (fWW) beneath bacteria (B) digesting the cell wall of an internodal cell of *Nitella flexilis*. Ch = chloroplast. (I) Wound walls (arrows) stained by Calcofluor at an alkaline region of a *C. corallina* internodal cell exposed to high light intensity (50 μmol m^{-2} s^{-1}) for 10 days. Bars are 1 μm (H), 10 μm (B, C, E, F), 40 μm (A, D), 50 μm (I) and 75 μm (G)

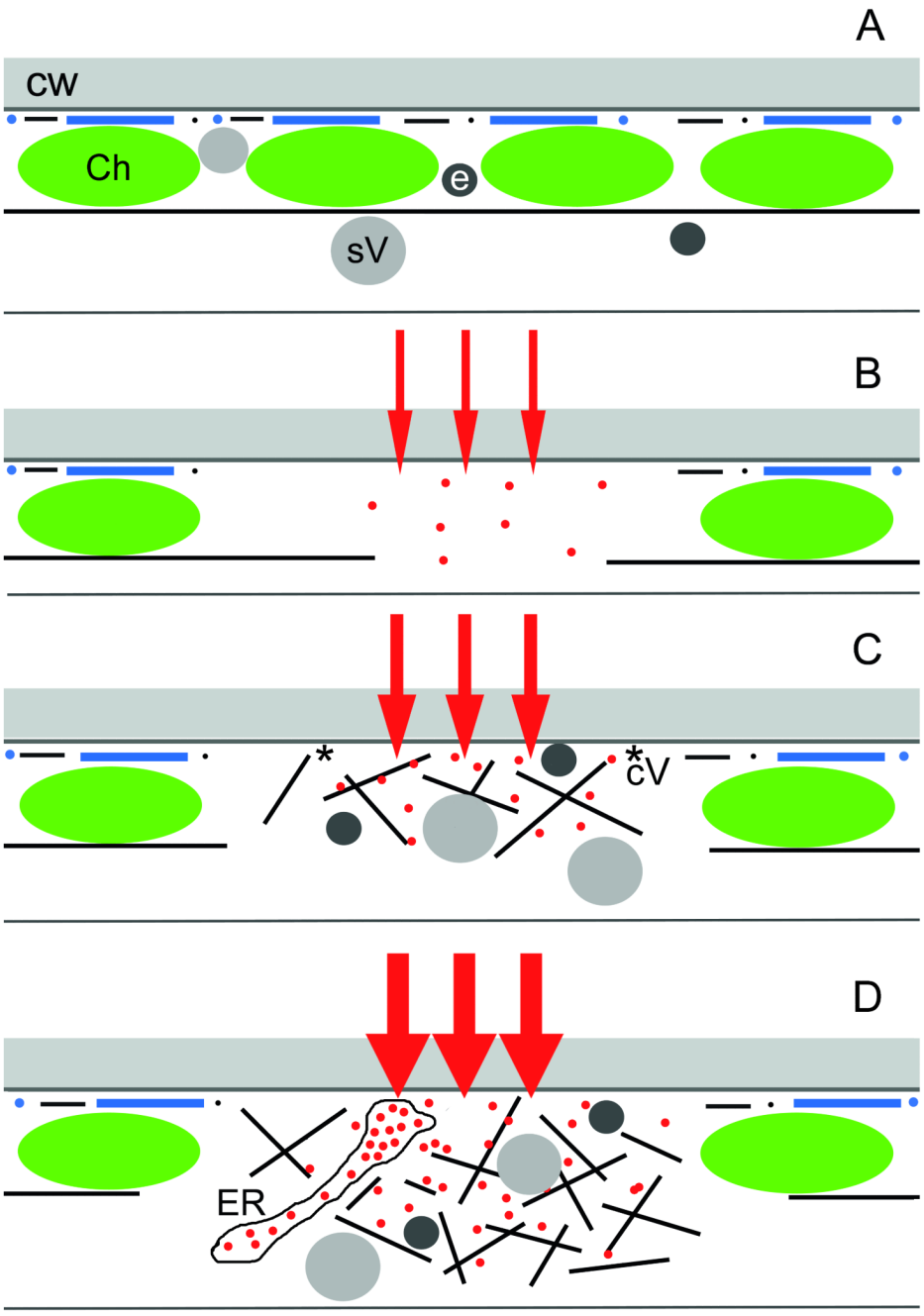

Fig. 6.

Schematic representation of early stages of wound responses in the cortex of characean internodal cells showing the major components involved, and the presumed Ca^{2+} influx. (A) In unwounded control cells and regions cortical actin filaments (black lines and dots) and microtubules (blue lines and dots) are present at the plasma membrane beneath the cell wall (CW). Continuous subcortical actin bundles are aligned along the stationary chloroplast (Ch) files. Secretory vesicles (sV) and putative endosomes (e) are present in the endoplasm and in the cortex. (B) Cortical window formation. Minor damage causes a small influx of external Ca^{2+} into the cytoplasm (red arrows and dots). This leads to the disassembly of the cortical cytoskeleton and of the subcortical actin bundles and to the detachment of chloroplasts. (C)

Deposition of a fibrillar wound wall. Moderate Ca^{2+} influx causes accumulation of secretory vesicles and endosomes, which move along a newly formed actin meshwork. The presence of coated vesicles (cV) indicates that vesicle fusion with the plasma membrane is coupled with endocytosis of excess membrane. (D) Deposition of an amorphous wound wall. High Ca^{2+} influx causes not only accumulation of vesicles but also of Ca^{2+}-loaded ER cisternae. Exocytosis of vesicles and ER takes place without endocytosis and excess membranes remain trapped within the amorphous wound wall.

Europe PMC Funders Author Manuscripts

Table 1

Characteristics of wound responses in characean internodal cells

	WINDOWS	FIBRILLAR WOUND WALLS	AMORPHOUS WOUND WALLS
typical treatment	local UV	$\geq 5\times10^{-2}$ M $CaCl_2$	Ca^{2+} ionophore A 23187 chlortetracycline
reorganization of actin cytoskeleton	minor	moderate	extensive (actin rings)
exocytosis	no	vesicles fuse with the plasma membrane	vesicles fuse with the plasma membrane, with other vesicles and with ER-cisternae
endocytosis	no	sufficient (numerous coated vesicles)	insufficient (few coated vesicles)
membrane residues in WW	none	absent	present
characteristic polysaccharide	none	crystalline cellulose	callose
DCB-treatment	no effect	alters wound wall structure	no difference
Ca^{2+} content of WW	no	low	high
notable changes in external ions and membrane potential	no	no	yes
presence of phenolics (autofluorescence)	none	low	high
time	ca 6 h	10-24 hours	$\geq$1 hour